

# NEW MAGNETIC SUPERCONDUCTORS: A TOY BOX FOR SOLID-STATE PHYSICISTS

Over the past decade, discussion of the interaction between superconductivity and magnetism has been overshadowed by the omnipresence of the oxide-based, high-temperature superconductors. But interest in the interaction between these two generally competing effects has a history that predates high- $T_c$  materials by several decades.<sup>1</sup> Starting with seminal work by Bernd Matthias and his coworkers, it was found that magnetic impurities strongly suppress superconductivity in pure elements and binary compounds. This rapid suppression of the superconducting transition temperature  $T_c$  was due to the local magnetic moment of the impurity preventing the formation of the spin-up/spin-down conduction-electron pairs that are responsible for superconductivity. The early measurements were made on dilute alloys, and for many solid-state physicists of the time, the quest was to find compounds in which superconductivity coexists with an ordered lattice of local magnetic moments.

The prize was found in the late 1970s with the discovery of two basic families of compounds:  $\text{RMO}_6\text{S}_8$  (as well as  $\text{RMO}_6\text{Se}_8$ ) and  $\text{RRh}_4\text{B}_4$ —in which R represents a rare earth element. In both of these families, superconductivity and local order of magnetic moments coexist for several members of the rare earth series. The importance of a rare-earth-bearing series is best summarized by a quote from Charles Kittel's *Introduction to Solid State Physics*: "The ions of the rare earth elements have closely similar chemical properties. . . . Their magnetic properties are fascinating: The ions exhibit a systematic variety and intelligible complexity." That is, by having several related compounds, with only the nature of the local moment varying, there is a chance of achieving a better understanding of how superconductivity and the local moments negotiate the nature of the low-temperature ground states in these compounds.

A few years ago, a new family of magnetic superconductors was discovered: the  $\text{RNi}_2\text{B}_2\text{C}$  series.<sup>2</sup> Physical,

**Rare earth nickel borocarbide compounds are rekindling interest in the decades-old question of how superconductivity and magnetism coexist, and some remarkable answers are emerging.**

Paul C. Canfield, Peter L. Gammel and David J. Bishop

earth elements dysprosium, holmium, erbium, thulium, lutetium and yttrium, giving experimenters lots of compounds to compare.

▷ The ratio of the superconducting ordering temperature to the antiferromagnetic ordering temperature,  $T_c/T_N$ , varies from much greater than 1 (11 K/1.5 K for  $\text{TmNi}_2\text{B}_2\text{C}$ ) to significantly less than 1 (6 K/10 K for  $\text{DyNi}_2\text{B}_2\text{C}$ ). (The antiferromagnetic ordering temperature is the temperature below which the local magnetic moments order into a state that has no net magnetization at zero temperature.) Thus the salient energy scales for antiferromagnetic order and superconductivity can be varied over a wide range and examined in two very different limits— $T_c > T_N$  and  $T_c < T_N$ .

▷ High-quality samples can be readily produced in single-crystal form (see figure 1 and the box on page 43), allowing for a much greater range of detailed thermodynamic, transport and microscopic measurements than is possible with polycrystalline samples.

Technologically, the wide range of experimental techniques that had been refined during the high- $T_c$  decade could be brought to bear on the new materials. And psychologically, it was nice to have a break from oxides and all the pleasures and problems associated with them.

Regardless of the reasons for the initial enthusiasm, the richness of physical effects that manifest themselves in the  $\text{RNi}_2\text{B}_2\text{C}$  series has far exceeded initial expectations. At this point, the  $\text{RNi}_2\text{B}_2\text{C}$  series contains many features that have individually been topics of keen interest over the past 20 years, all wrapped up in one simple crystal structure. These features include magnetic superconductors,<sup>2</sup> nonlocality in superconductors,<sup>3</sup> soft (low-energy) phonons and Fermi surface nesting,<sup>4</sup> square vortex lattices and transitions in the vortex lattice symmetry,<sup>5</sup> heavy-fermion ground states (see the box on page 45),<sup>6</sup> ordering of highly anisotropic local moments and clear angular dependencies of field-stabilized states (metamagnetism).<sup>7</sup> This series of compounds has truly become a new toy box

PAUL CANFIELD is an associate professor of physics and astronomy at Iowa State University in Ames, Iowa, and a physicist at the university-operated Ames Laboratory. PETER GAMMEL and DAVID BISHOP are members of technical staff at Bell Laboratories, Lucent Technologies, in Murray Hill, New Jersey.





FIGURE 1. SINGLE CRYSTAL of  $\text{LuNi}_2\text{B}_2\text{C}$  grown from molten  $\text{Ni}_2\text{B}$ . The mass of this magnetic superconductor is about 1 gram.

for solid-state physicists.

In this article, we highlight some of the more basic discoveries, as well as some of the currently hot areas of research, associated with the  $\text{RNi}_2\text{B}_2\text{C}$  compounds, where  $\text{R} = \text{Gd-Lu}$  and  $\text{Y}$ . This article is a midgame commentary, not a postgame review: We are looking at an area of ongoing research. Space limitations allow us to sample this research, but not to give a full review of all work.

## Discovery: "Care and diligence bring luck"

During the waning months of 1993, two groups were chasing small but intriguing traces of superconductivity in yttrium-nickel-boron ternary compounds, as Chandan Mazumdar and his coworkers reported.<sup>8</sup> In January 1994, in *Physical Review Letters*,<sup>9</sup> Radhakrishnan Nagarajan and his coworkers identified a yttrium-nickel-boron-carbon quaternary alloy as having a superconducting transition temperature of 12 K. In the same month, Robert Cava, Theo Siegrist and their colleagues published a series of letters to *Nature*<sup>2</sup> reporting superconductivity with a  $T_c$  of 23 K in the yttrium-palladium-boron-carbon quaternary alloy and identifying a series of  $\text{RNi}_2\text{B}_2\text{C}$  compounds as having  $T_c$  as high as 16.6 K. In addition to identifying the stoichiometry of this series, the crystal structure was also reported.

The manner in which these compounds were discovered shows how equal parts of focused research and the proper interpretation of serendipity can lead to the discovery of important new materials. Cava made many attempts to reproduce Mazumdar's results, even trying with other transition metals instead of nickel. In one  $\text{Y-Pd-B}$  sample, he saw less than 1% superconductivity. In an attempt to have the sample cool a little more slowly, Cava placed the pressed pellet of elements on a carbon slab, hoping that it would act as a thermal barrier and lead to a slower cooling rate after melting. In this case over 10% of the

sample was superconducting, but he noticed that there was some evidence of attack on the carbon slab: A pit had been eaten away by the molten sample.

It thus became clear that carbon may well be the missing key. (Indeed carbon can be an impurity in nickel, palladium and boron.) Cava estimated how much carbon had been removed from the slab, tried a quaternary melt of  $\text{Y-Pd-B-C}$  and discovered that the superconducting phase was indeed a quaternary compound. Once it was clear that carbon was the missing element, it was added to the  $\text{Y-Ni-B}$  ternary mix. The superconducting phase was found<sup>2</sup> to be  $\text{YNi}_2\text{B}_2\text{C}$ . In addition to  $\text{YNi}_2\text{B}_2\text{C}$  and  $\text{LuNi}_2\text{B}_2\text{C}$ , several moment-bearing members of the  $\text{RNi}_2\text{B}_2\text{C}$  series also manifest superconductivity. The thermodynamic stability of the  $\text{RNi}_2\text{B}_2\text{C}$  series (that is, the relative ease of sample preparation), as well as the extent of superconductivity in the series ( $T_c > 0.3$  K for  $\text{R} = \text{Y, Lu, Tm, Er, Ho, Dy}$ ), have made the series a focus of attention for many research groups.

## Basic properties

The crystal structure of the  $\text{RNi}_2\text{B}_2\text{C}$  compounds is a variant of the  $\text{ThCr}_2\text{Si}_2$  structure,<sup>2</sup> which is one of the more ubiquitous structures for ternary intermetallic compounds. The structure is a layered one with  $\text{R-C}$  sheets separating slabs of  $\text{Ni}_2\text{B}_2$ , repeating along the crystallographic  $c$  axis like an endless Dagwood sandwich. The  $\text{R}$  site is a point of tetragonal symmetry, which leads to the magnetic moments being either axial or planar at low temperatures.

Band-structure calculations<sup>10</sup> have yielded a wealth of insight into this series, predicting that

- ▷ The materials have nearly isotropic electrical resistivity.
- ▷ There is a sharp, local maximum in the electronic density of states near the Fermi surface.
- ▷ There is a maximum in the generalized electronic



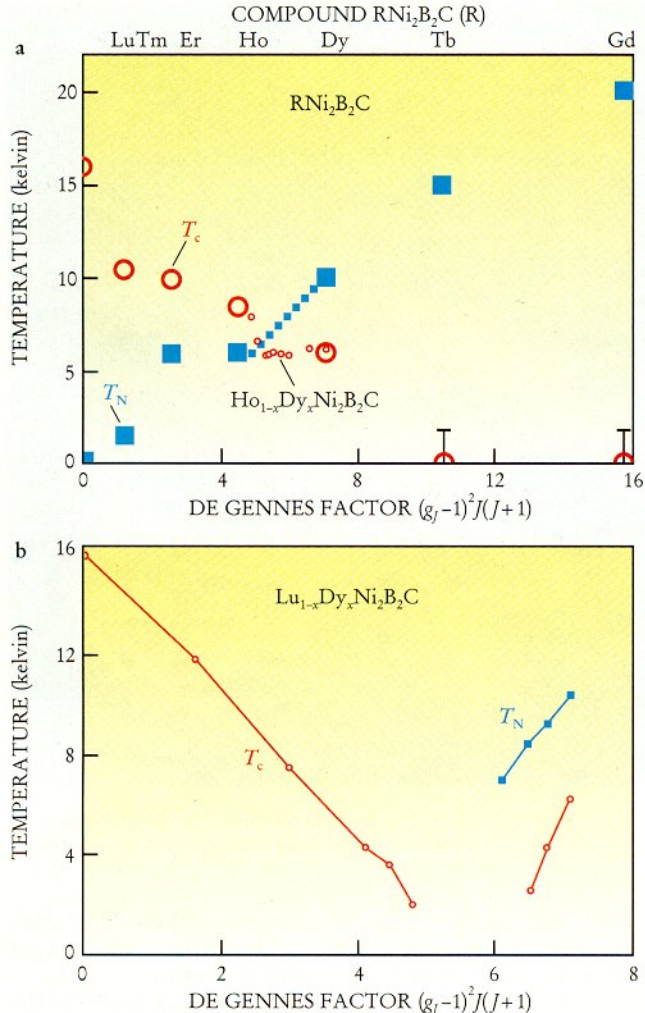


FIGURE 2. KEY TEMPERATURES for various rare earth nickel borocarbide compounds. **a:** Superconducting transition temperature  $T_c$  (red) and antiferromagnetic ordering temperature  $T_N$  (blue) plotted as functions of the de Gennes factor for the compounds  $RNi_2B_2C$  indicated on the upper axis. Small data points are for the series of compounds  $Ho_{1-x}Dy_xNi_2B_2C$ . **b:**  $T_c$  and  $T_N$  versus the de Gennes factor for the compounds  $Lu_{1-x}Dy_xNi_2B_2C$ .

stoichiometry, a tetragonal crystal structure and the possibility of studying the interaction between superconductivity and local moment magnetism.

## Low-field properties

The interaction between rare earth magnetic moments in a metal (known as the Ruderman-Kittel-Kasuya-Yosida, or RKKY interaction) is mediated by the conduction electrons. For relatively simple models of intermetallic compounds,<sup>1</sup> this interaction leads to a linear dependence of the antiferromagnetic ordering temperature  $T_N$  on two terms: the coupling between the conduction electrons and the local moments  $I$ , and the de Gennes factor  $dG$ , which is itself a function of the quantum numbers  $L$ ,  $S$  and  $J$  associated with the unfilled 4f electron shell of the rare earth ion:

$$T_N \propto I^2 dG,$$

where  $dG = (g_J - 1)^2 J(J + 1)$  and the Lande  $g$  factor

$$g_J = 1 + \{[J(J + 1) + S(S + 1) - L(L + 1)]/[2J(J + 1)]\}.$$

In a similar manner, the suppression of  $T_c$  by uncorrelated magnetic moments is linear in  $dG$ :

$$\Delta T_c \propto -I^2 N(\epsilon_F) dG.$$

Therefore, if  $I$  and  $N(\epsilon_F)$  can be considered roughly constant across a series of compounds, then both  $T_N$  and  $\Delta T_c$  will have a linear dependence on the de Gennes factor. This is an example of the systematic variety and intelligible complexity, mentioned above, that the rare earth series offers.

The suppression of  $T_c$  is due to the magnetic moments preventing the formation of spin-up/spin-down Cooper pairs and is referred to as magnetic pair breaking. For an analogy, one can think of two slalom skiers who wish to ski next to each other as they go down a hill. In the absence of moguls (bumps on the ski slope), this activity would be easy for the skiers. However, with many moguls randomly placed on the slope, it would be quite hard for our skiers to stay together, as each would be negotiating different bumps at different times. In our analogy, the moguls are the magnetic moments with their density, height and size influencing the amount of "depairing." In the real system, the density and strength of the pair breaking are represented by the de Gennes factor.

The features that first attracted attention to the  $RNi_2B_2C$  series were the relatively high  $T_c$  values and the persistence of superconductivity in the moment-bearing members ( $R = Dy, Ho, Er$  and  $Tm$ ). Figure 2a shows values of  $T_c$  and  $T_N$  for the heavy rare earth members of the series plotted as a function of rare earth and as a function of de Gennes factor. As anticipated,  $T_N$  has a roughly linear dependence on the de Gennes factor, and to a lesser extent the suppression of  $T_c$  appears to have a roughly linear dependence on  $dG$  too.

A clear feature in figure 2a is the crossing of  $T_c$  and  $T_N$  between  $HoNi_2B_2C$  and  $DyNi_2B_2C$ . Indeed,  $DyNi_2B_2C$  is one of only a few fully local moment compounds that

susceptibility  $\chi(q)$  for finite wavevector  $q$ .

Each of these predictions has been borne out experimentally. The last one manifests itself both as a common magnetic ordering wavevector (in materials with  $R = Er, Ho, Tb$  and  $Gd$ ) and as the wavevector about which a dramatic phonon softening is centered (in materials with  $R = Lu, Y, Er$  and  $Ho$ ). Recently, specific interest has focused on the fact that, at low temperatures, this phonon mode has an energy comparable to the superconducting energy gap. This match has made it possible to observe the superconducting energy gap by means of inelastic neutron scattering.<sup>4</sup>

In many ways, work on  $LuNi_2B_2C$  typifies the direction that researchers were following 20 years ago. Using simple Bardeen-Cooper-Schrieffer theory, the superconducting transition temperature is expected to be

$$T_c \propto \Theta_D \exp(-1/\lambda N(\epsilon_F)),$$

where  $\Theta_D$  is the Debye temperature (a measure of the frequency of atomic vibration),  $N(\epsilon_F)$  is the density of electronic states at the Fermi surface and  $\lambda$  is the electron-phonon coupling. Compounds in the  $RNi_2B_2C$  series have a moderately large  $\lambda$  and a moderately large  $N(\epsilon_F)$ , and the light elements B and C offer the possibility of a fairly large  $\Theta_D$ ; therefore, one can expect a relatively high  $T_c$ . In this manner, nonmagnetic  $LuNi_2B_2C$  and  $YNi_2B_2C$  are very similar to intermetallic superconductors such as  $V_3Si$  with pre-oxide high  $T_c$ 's. The primary differences are that, for the  $RNi_2B_2C$  series, there is a well-defined



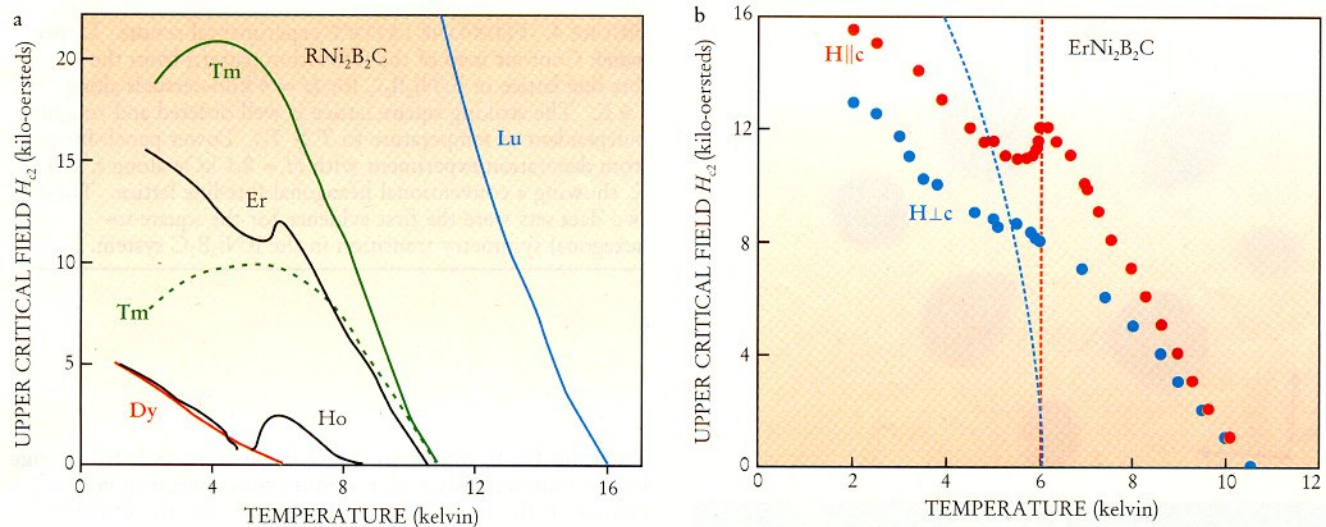


FIGURE 3. UPPER CRITICAL FIELD  $H_{c2}$  for superconductivity, plotted as a function of temperature for various rare earth (R) nickel borocarbide compounds  $RNi_2B_2C$ . **a:**  $H_{c2}$  for  $R = Lu, Tm, Er, Ho$  and  $Dy$ . The solid lines are for the applied field  $H$  along the axis of least sublattice magnetization. The dashed line for  $R = Tm$  is for the field applied along the axis of greatest sublattice magnetization. **b:**  $H_{c2}$  for  $R = Er$  with  $H||c$  (red) and  $H\perp c$  (blue). The dashed lines are part of the  $H$ - $T$  phase diagram for the magnetically ordered state.

has  $T_N > T_c$  and has a clear separation of  $T_c$  and  $T_N$ , with both temperatures being easily accessible.<sup>11</sup> To study this crossover from  $T_c > T_N$  to  $T_c < T_N$ , we grew a series of pseudoquaternary samples.  $T_c$  and  $T_N$  data for the  $(Ho_{1-x}Dy_x)Ni_2B_2C$  series are shown as the smaller symbols in the figure.<sup>12</sup> Whereas the  $T_N$  data continue to increase linearly with  $dG$ , as seen for the  $RNi_2B_2C$  compounds, the  $T_c$  data manifest a clearly nonlinear dependence on  $dG$ . Specifically, as soon as  $T_c$  crosses below  $T_N$ , dependence of  $T_c$  on  $dG$  virtually disappears.

When we first collected these data, we were impressed and startled by the behavior of  $T_c$ . The knee-jerk reaction of a confused experimenter (at least in our group) is to make another, one hopes simpler, measurement. So we

examined the  $(Lu_{1-x}Dy_x)Ni_2B_2C$  series to see if a step backward to a nonmagnetic/magnetic dilution would simplify matters.<sup>12</sup> Figure 2b shows  $T_c$  and  $T_N$  data for this series. On the  $LuNi_2B_2C$  side (small  $dG$  factor), where  $Dy$  is acting like a dilute paramagnetic impurity,  $T_c$  is suppressed in a manner similar to that seen for dilute  $Ho$  and  $Gd$  impurities.<sup>12</sup> The one point worth noting is that the dilute  $Dy$  data indicate that there will be no superconducting transition in pure, paramagnetic  $DyNi_2B_2C$ : The data extrapolate to  $T_c = 0$  K before pure  $DyNi_2B_2C$  is reached. This is, of course, not the case: Pure  $DyNi_2B_2C$  orders antiferromagnetically at  $T_N = 10$  K and superconducts with a  $T_c = 6$  K. The data on the  $Dy$ -rich (higher  $dG$  factor) side of figure 2b are far more interesting:  $T_c$

## Crystal Growth

Single crystals of intermetallic compounds can be grown in a variety of ways. Conventional (and industrial) methods use moderate-to-large temperature gradients to grow sizable crystals of congruently or near-congruently melting compounds. A congruently melting compound is one that simply melts at a given temperature. This property allows a temperature gradient to include both the liquid and solid phases. However, the majority of intermetallic compounds, including  $RNi_2B_2C$ , are incongruently melting. This means that there is a finite (and often large) temperature difference between the liquid and solid phases. For incongruently melting compounds, the conventional techniques are difficult to use at best.

Another method of growing single crystals is to grow them from a high-temperature solution. One of the advantages of solution growth is that it works for both congruently and incongruently melting compounds. A major disadvantage is that one must discover a solvent and a temperature range for growth, often by trial and error. The solvent must be a liquid at temperatures below the melting or decomposition point of the desired compound and must not lead to the formation of secondary phases, at least over some limited (but tractable) temperature range.

For a quaternary system such as  $RNi_2B_2C$ , there are many

possibilities for solvents. Examples include aluminum fluxes, gallium fluxes and binary compounds such as  $RNi$ ,  $RC$  and  $NiB$ . In March 1994, after two months of trial and error, we found that growth of  $RNi_2B_2C$  out of excess  $Ni_2B$  works very well. In retrospect, this was the obvious choice. Nickel is one of several transition metals that, when mixed with boron, has a remarkably low melting point. By slowly cooling a mixture of  $RNi_2B_2C$  and  $Ni_2B$  from 1500 °C to 1200 °C over the course of several days, single crystals of up to 0.8 gram have been grown. (See figure 1.) In our lab, we have been able to grow sizable ( $10 \times 10 \times 1$  mm) single crystals for  $R =$  terbium-lutetium and yttrium, as well as smaller single crystals for  $R =$  neodymium, samarium and gadolinium.

The ready availability of single-crystal samples so early in the game has allowed experimenters to appreciate the profound (magnetic) and subtle (electronic) anisotropies in these materials. Large  $^{11}B$ -enriched crystals have made it possible to use neutron scattering to study the magnetic and vortex ordering, as well as the phonon modes. In addition, single crystals have made possible the measurement of single-phase, low-strain, high-purity samples from virtually the onset of research on these compounds.



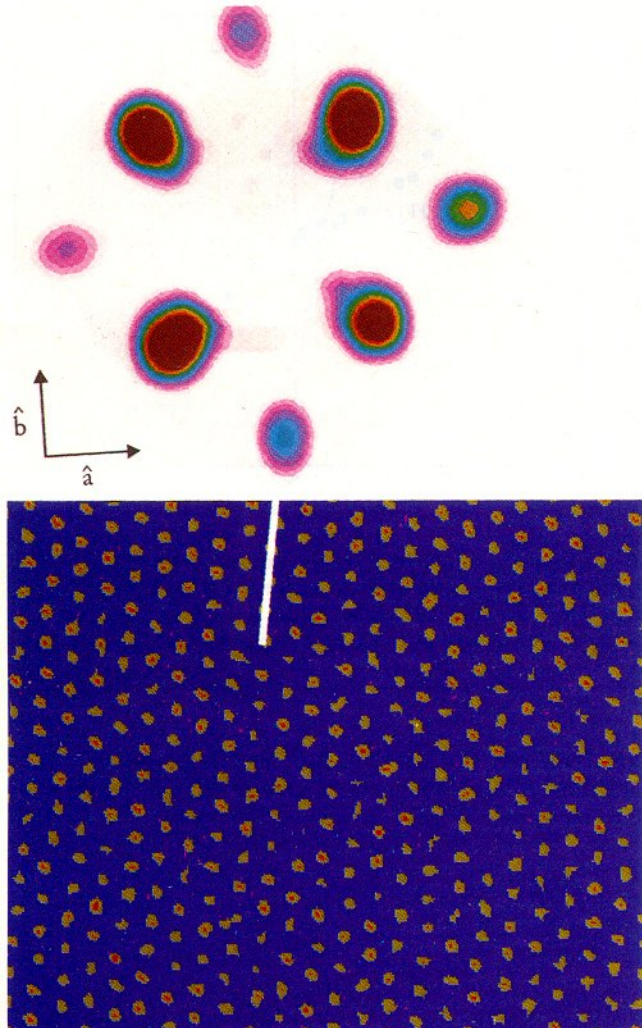


FIGURE 4. FLUX-LINE LATTICE experimental results. Upper panel: Contour map of the diffraction pattern from the flux-line lattice in  $\text{ErNi}_2\text{B}_2\text{C}$  for  $H = 4$  kilo-oersteds along  $c$ , at 1.6 K. The striking square lattice is well ordered and roughly independent of temperature to  $T > T_N$ . Lower panel: Image from decoration experiment with  $H = 0.1$  kOe along  $c$ , at 4.2 K, showing a conventional hexagonal flux-line lattice. These two data sets were the first evidence for the square-to-hexagonal symmetry transition in the  $\text{RNi}_2\text{B}_2\text{C}$  system.

Thus, as Ho is added to  $\text{DyNi}_2\text{B}_2\text{C}$ , there is little change in the magnetically ordered state and therefore very little change in the degree of pair breaking. On the other hand, nonmagnetic Lu is very different from magnetic Dy. Lu is a magnetic zero in the Dy sublattice. As Lu is added to  $\text{DyNi}_2\text{B}_2\text{C}$ ,  $T_N$  is suppressed and the magnetically ordered state below  $T_N$  is significantly changed. In essence, additions of small amounts of nonmagnetic Lu increase the capability of the remaining, less correlated Dy to act as a magnetic pair breaker.

## Effects of applied magnetic field

The effects of local moment magnetism on the superconducting state can be seen even more clearly in  $H$ - $T$  phase diagrams, specifically in data on the upper critical field  $H_{c2}(T)$ , which is the magnetic field above which bulk superconductivity ceases to exist. Figure 3a presents data for  $R = \text{Lu}, \text{Tm}, \text{Er}, \text{Ho}$  and Dy. As can be seen, there is a general reduction of the upper critical field as  $T_c$  is suppressed. In addition, there are a wide variety of temperature dependencies associated with the paramagnetic and ordered states of the rare earth sublattice.  $\text{TmNi}_2\text{B}_2\text{C}$  and  $\text{ErNi}_2\text{B}_2\text{C}$  clearly exemplify these two regimes.<sup>13</sup>

$\text{TmNi}_2\text{B}_2\text{C}$  is a particularly good system in which to see the effects of the paramagnetic sublattice, because there is a large temperature range between  $T_c = 11$  K and  $T_N = 1.5$  K;  $T_N/T_c = 0.14$ . There are two features of specific interest apparent in the upper critical field data for  $\text{TmNi}_2\text{B}_2\text{C}$  as shown in figure 3a: its anisotropy and the form of its temperature dependence. The anisotropy in  $H_{c2}$  can be understood qualitatively by thinking of the internal field—the field experienced by the conduction electrons. The larger the sublattice magnetization, the larger the internal field on the conduction electrons, and the sooner superconductivity is killed. For all measured temperatures,  $H_{c2}$  for  $H \parallel c$  (dashed line) is lower than  $H_{c2}$  for  $H \perp c$  (solid line). This is consistent with the anisotropy of the Tm sublattice, which has a larger magnetization for  $H \parallel c$  than for  $H \perp c$ . The broad maxima in  $H_{c2}$  are associated with the suppression of  $H_{c2}$  by the temperature-dependent Tm sublattice magnetization,<sup>13</sup> which is essentially proportional to  $1/T$  at these temperatures. For  $T < 5$  K, the temperature dependence of the upper critical field is dominated by this suppression.

Figure 3b shows anisotropic upper critical field data for  $\text{ErNi}_2\text{B}_2\text{C}$ . Again, there are two clear anisotropies in these data: in  $H_{c2}$ 's magnitude and in its temperature dependence. While the physics behind the difference in magnitude is the same as that described for  $\text{TmNi}_2\text{B}_2\text{C}$ , the anisotropic temperature dependence comes from a different effect. For  $H \parallel c$ , there is a sharp decrease in  $H_{c2}$  just below  $T_N$ . This feature is associated with an increase

is suppressed by the addition of dilute, nonmagnetic, Lu impurities.

While at first these data appeared to be quite surprising, they are actually rather easy to understand qualitatively. Going back to our analogy of the skiers, remember that randomly placed moguls acted as pair breakers, making it hard for the skiers to stay together on the slope. However, if the moguls are ordered, or placed in regular positions, then once again the skiers can stay together, as each is negotiating an identical mogul at the same time as the other skier and will experience identical delays going down the hill. The ordered moguls correspond to the situation of the magnetic impurities ordering below  $T_N$ .

Physically speaking, in the paramagnetic regime ( $T > T_N$ ), the pair breaking can be thought of as spin-flip scattering between a conduction electron and a local magnetic moment, leading to the suppression of  $T_c$ . On the other hand, in the magnetically ordered state it is not spin-flip scattering of an isolated moment, but interaction with some kind of collective mode that gives rise to the pair breaking. Therefore, the apparently counterintuitive situation for  $T_c < T_N$ , where nonmagnetic impurities lower  $T_c$  and magnetic impurities have little effect, must be understood by determining what these substitutions do to the collective modes of the antiferromagnetic ground state.

In the case of  $\text{HoNi}_2\text{B}_2\text{C}$  and  $\text{DyNi}_2\text{B}_2\text{C}$ , the Ho and Dy moments are virtually the same (in magnitude and anisotropy) and they order magnetically at low temperatures with the same simple, antiferromagnetic structure.



in pair breaking for temperatures near  $T_N$ . Such an increase in pair breaking has been predicted<sup>1,14</sup> for compounds in which the wavevector of the magnetic ordering is one at which there is a maximum in  $\chi(q)$ ,<sup>10</sup> as is the case for  $\text{ErNi}_2\text{B}_2\text{C}$ . On the other hand, there is no such sharp feature for  $H \perp c$ .

There are two possible explanations for this difference. The first is that, for  $H \perp c$ ,  $T_N$  is suppressed as the applied field is increased. This is shown by the dashed lines in figure 3b. Therefore, as  $H$  approaches  $H_{c2}$ ,  $T_N$  is reduced, and what was a sharp feature when  $T_N$  was independent of applied field for  $H \parallel c$  is now a broadened point of inflection. The second possibility, which is both somewhat more quantitative and intriguing, is that, for some  $H < H_{c2}$ , there is a change in the ordering wavevector to a value for which there is no maximum in  $\chi(q)$ , thereby avoiding the increase in pair breaking at  $T_N$ . Indeed, this hypothesis is consistent with studies<sup>7</sup> of metamagnetism in  $\text{ErNi}_2\text{B}_2\text{C}$ , which show small steps in the field-dependent magnetization for fields of less than  $H_{c2}$ .

$\text{HoNi}_2\text{B}_2\text{C}$  and  $\text{DyNi}_2\text{B}_2\text{C}$  (figure 3a) have more isotropic  $H_{c2}(T)$  curves. This property is associated with the fact that  $H_{c2}$  for these compounds is lower than that seen for  $\text{ErNi}_2\text{B}_2\text{C}$  or  $\text{TmNi}_2\text{B}_2\text{C}$ , leading to smaller effects due to either sublattice magnetization or (in the case of  $\text{HoNi}_2\text{B}_2\text{C}$ ) suppression of  $T_N$  by the applied field.  $\text{HoNi}_2\text{B}_2\text{C}$  also has a suppression of  $H_{c2}$  near  $T_N$ , but this behavior is complicated by a cascade of different ordered states existing between 5 and 6 K. On a gross level the suppression is similar in magnitude to that seen in  $\text{ErNi}_2\text{B}_2\text{C}$ , and it very likely has a similar origin.

## Flux-line lattice

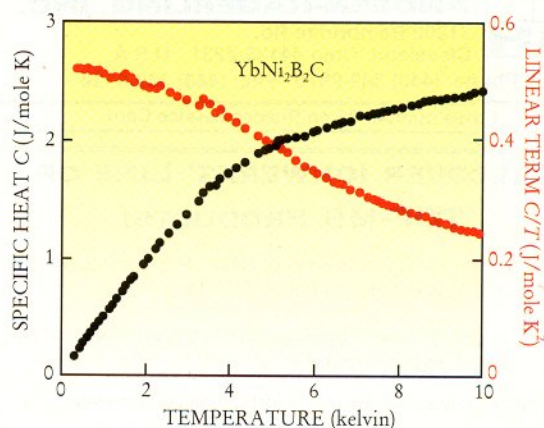
Members of the  $\text{RNi}_2\text{B}_2\text{C}$  family have relatively high upper critical fields (figure 3) but relatively low lower critical fields. A typical lower critical field  $H_{c1}$  (the applied field above which the magnetic field penetrates the sample) is on the order of 0.1 kilo-oersted ( $T = 2$  K) for most of the members. That is to say, many of the properties of the superconducting state are determined by the array of quantized magnetic flux lines that permeate the material over almost the entire  $H$ - $T$  plane. This array is known alternatively as either the flux-line lattice or the vortex lattice. Many of the same characteristics that make their normal and superconducting properties quite exotic also conspire to produce vortex matter in these materials completely unlike anything we have ever seen before.<sup>5</sup>

Figure 4 shows two images taken of the flux-line lattice<sup>5</sup> in  $\text{ErNi}_2\text{B}_2\text{C}$  for  $H \parallel c$ . The lower panel shows a low-field real-space image, obtained by means of magnetic decoration, of the flux-line lattice in this compound taken at 4.2 K and 0.1 kOe. What one sees is a rather unremarkable hexagonal lattice oriented along the crystal [100] direction (white line), with a conventional value for the flux quantum  $\phi_0 = hc/2e$ . However, shown in the upper panel is a small-angle neutron scattering  $k$ -space image of the flux-line lattice in this same compound at a field of 4 kOe and a temperature of 1.6 K. Clearly, the lattice is a square, and it is oriented along the [110] direction. This is the first example of a square vortex lattice in a high- $H_{c2}$ , low- $H_{c1}$  superconductor, although it appears to be a ubiquitous feature of the borocarbide superconductors and has been detected in other members of the series by a variety of techniques, including scanning tunnelling microscopy.<sup>15</sup> Taken together, these two images imply that there exists a square-to-hexagonal symmetry transition for the flux-line lattice in this compound for applied fields between 0.1 and 4.0 kOe.

Detailed studies of the flux-line lattice in  $\text{ErNi}_2\text{B}_2\text{C}$  have now given us a rather complete picture of this

## A New Heavy Fermion

$\text{YbNi}_2\text{B}_2\text{C}$  is one of very few known ytterbium-based heavy-fermion compounds and is currently the most likely candidate to be the canonical example of this class of materials that exhibit very strong electron-electron correlations below a characteristic temperature known as the Kondo temperature  $T_K$ . In simple models, these correlations are interpreted as being due to a large renormalized electron mass, hence the term "heavy fermion." While there are several cerium-based heavy fermions, Yb-based examples have remained relatively rare. Consequently, it has been difficult to make comparisons of the Ce,  $4f^1$  (electron) and Yb,  $4f^{13}$  (hole) systems. (The superscripts 1 and 13 indicate the number of electrons in the  $4f$  shell of the trivalent rare earth ion.) Unlike the other known<sup>17</sup> Yb-based heavy-fermion material  $\text{YbBiPt}$ ,  $\text{YbNi}_2\text{B}_2\text{C}$  has a very clear segregation of energy (temperature) scales:  $T_c$ ,  $T_N < 0.3$  K,  $T_K \approx 10$  K, and the energy separation between the ground-state crystalline electric field levels and the first excited CEF level  $kT_{\text{CEF}} > 9$  meV ( $\approx 100$  K).<sup>6</sup> This places the Kondo temperature  $T_K$  in an energetic wasteland and allows for the clean examination of correlated electron effects in  $\text{YbNi}_2\text{B}_2\text{C}$ . As  $T$  is lowered through  $T_K$ , the entropy associated with the local magnetic moment degeneracy is transferred to the conduction electrons, giving rise to the temperature-dependent specific heat  $C(T)$  of  $\text{YbNi}_2\text{B}_2\text{C}$  (see figure), which has a low-temperature linear term  $C(T)/T$  that saturates at 530 mJ/K<sup>2</sup>-mole.



SPECIFIC HEAT of  $\text{YbNi}_2\text{B}_2\text{C}$ . At low temperatures the specific heat varies linearly with temperature (black data points) and the ratio of specific heat to temperature saturates at 530 mJ/K<sup>2</sup>-mole (red data points).

square-to-hex transition. Experiments have shown that it is a continuous transition that occurs at roughly 0.5 kOe. Theoretical work has shown that the transition arises because of a steric interaction between vortices with slightly noncircular (squareish) cross sections that are due to the underlying crystalline symmetry.<sup>3</sup> The transition field is a function of two length scales: the electron mean free path and the superconducting coherence length. By doping these compounds and decreasing the ratio of the electronic mean free path to the superconducting coherence length, the square-to-hexagonal transition should be moved to higher fields.<sup>16</sup> Indeed, this effect has recently been observed in a small-angle neutron scattering experiment.

As a last note on flux-line lattice research, recent



## STOP MANUALLY BALANCING!



The Model 2902A Analytical Balance is the most accurate, precise, and reliable balance available.

**SUPER-ENGINEERING**  
**AUTOMATIC CALIBRATION**  
**AUTOBALANCE**

### APPLICATIONS INCLUDE:

- Low- and high-temperature studies
- Cryogenic measurements
- Fluid vapor studies
- Studies on Oxidation, Thermal Expansion, Pressure, AC Resistance, Contaminants, Thickness of Films, or Dielectrics
- Monitoring of Chemical Reactions, and Direct humidity

### Specifications of Model 2902A with Option B:

- Accuracy of 3 ppm
- Stability better than 0.5 ppm/year
- Resolution of 0.5 micrograms and 0.07 ppm
- Temperature coefficient of 0.01 ppm/°C
- Conductivity as low as  $3 \times 10^{-10}$  mhos/cm
- Dissipation as low as  $1.5 \times 10^{-10}$  W/cm
- RS-232C and RS-485 interfaces included
- **COMPREHENSIVE 300+ PAGE MANUAL**

FOR MORE INFORMATION, CONTACT:

**ANDERSON-HAGERLING, INC.**  
 31200 Bainbridge Rd.  
 Cleveland, Ohio 44139-2231 U.S.A.  
 Phone: (440) 349-0370 Fax: (440) 349-0399

Circle number 22 on Reader Service Card

## DISCOVER IONWERKS' LINE OF TOF-MS PRODUCTS:

- Reflections and HV electronics for SIMS, Mass Spectrometry of Resolved Ions (MSRI), and other TOF-MS
- Four channel, 625 psec Time-to-Digital Converter plus 16 Mbit Histogram Memory for under \$10K
- Scalable, scalable 4 anode multi-channel plate ion detectors
- HV Supplies for ion beam pulsing, steering, and focusing
- Complete custom ion scattering systems

### FEATURING:



**REFLECTRON MASS SPECTROMETER**  
**1997 R&D 100 AWARD WINNER**

- Real-time real-time surface analysis during the ion growth or evaporation cycle

- Average full-scale resolution of 10,000 from SIMS, IMA, and Mass Spectrometry of Resolved Ions (MSRI)

To learn more about Ionwerks, visit us at  
**AVS Booth 250**

or  
 browse our website at  
**www.ionwerks.com**

**IONWERKS**

247 Science Bldg. 2F  
 Houston, TX 77056  
 (713) 524-8889  
 fax (713) 524-8735  
 www.ionwerks.com

small-angle neutron scattering data on  $\text{TmNi}_2\text{B}_2\text{C}$  have revealed a series of flux-line lattice structural transitions that seem to indicate a direct coupling between the symmetry of the magnetic structures and the symmetry of the flux-line lattice.<sup>5</sup> If, as is our belief, the changes in the magnetic structure actually drive the flux-line lattice structural changes, then  $\text{TmNi}_2\text{B}_2\text{C}$  provides the clearest example to date of the interaction between local moments and the flux-line lattice.

## Future work

The  $\text{RNi}_2\text{B}_2\text{C}$  series has been a surprisingly fertile ground for research over the past four years. During this period the series has provided an excellent study of the interaction between magnetism and superconductivity and also has opened up new areas of research. Up to now the series has been like a new ball of string for a kitten—wildly entertaining to bat around and see what happens. The potential to use the data collected over the past four years to reexamine the physics of the interplay between magnetism and superconductivity should be apparent. Now, though, the hard part begins: Can our empirical understanding of this series be translated into an improved theoretical understanding of magnetic superconductors? Addressing this question will be the challenge for the next several years.

Paul Canfield's work is supported by the U.S. Department of Energy, Office of Basic Energy Sciences.

## References

1. For reviews, see the following: K. Buschow, E. Wohlfarth, eds., *Ferromagnetic Materials*, Elsevier, Amsterdam (1990), chap. 6. M. B. Maple, O. Fisher, eds., *Superconductivity in Ternary Compounds II*, Springer-Verlag, Berlin (1982).
2. R. J. Cava *et al.*, *Nature* **367**, 146 (1994). R. J. Cava *et al.*, *Nature* **367**, 252 (1994). T. Siegrist *et al.*, *Nature* **367**, 254 (1994).
3. V. G. Kogan *et al.*, *Phys. Rev. B* **55**, R8693 (1997). V. G. Kogan *et al.*, *Phys. Rev. Lett.* **79**, 741 (1997).
4. P. Dervenagas *et al.*, *Phys. Rev. B* **53**, 8506 (1996). C. Stassis *et al.*, *Phys. Rev. B* **55**, R8678 (1997). M. Bullock *et al.*, *Phys. Rev. B* **57**, 7916 (1998).
5. U. Yaron *et al.*, *Nature* **382**, 236 (1996). M. R. Eskildsen *et al.*, *Phys. Rev. Lett.* **78**, 1968 (1997). D. McK. Paul *et al.*, *Phys. Rev. Lett.* **80**, 1517 (1998). M. R. Eskildsen *et al.*, *Nature* **393**, 242 (1998).
6. A. Yatskar *et al.*, *Phys. Rev. B* **54**, R3772 (1996). S. K. Dhar *et al.*, *Solid State Commun.* **98**, 985 (1996). S. L. Bud'ko, P. C. Canfield, A. Yatskar, W. P. Beyermann, *Physica B* **230-32**, 859 (1997). R. Sala, F. Borsa, E. Lee, P. C. Canfield, *Phys. Rev. B* **56**, 6195 (1997).
7. P. C. Canfield *et al.*, *Phys. Rev. B* **55**, 970 (1997). P. C. Canfield, S. L. Bud'ko, *Journal of Alloys and Compounds* **262-63**, 169 (1997). P. C. Canfield, S. L. Bud'ko, B. K. Cho, *Physica C* **262**, 249 (1996).
8. C. Mazumdar *et al.*, *Solid State Commun.* **87**, 413 (1993).
9. R. Nagarajan *et al.*, *Phys. Rev. Lett.* **72**, 274 (1994).
10. L. F. Mattheiss, *Phys. Rev. B* **49**, 13 279 (1994). W. E. Pickett, D. J. Singh, *Phys. Rev. Lett.* **72**, 3702 (1994). J. Y. Rhee, X. Wang, B. N. Harmon, *Phys. Rev. B* **51**, 15 585 (1995).
11. B. K. Cho, P. C. Canfield, D. C. Johnston, *Phys. Rev. B* **52**, R3844 (1995). C. V. Tomy *et al.*, *Phys. Rev. B* **52**, 9186 (1995).
12. B. K. Cho, P. C. Canfield, D. C. Johnston, *Phys. Rev. Lett.* **77**, 163 (1996).
13. B. K. Cho *et al.*, *Phys. Rev. B* **52**, 3676 (1995). B. K. Cho *et al.*, *Phys. Rev. B* **52**, 3684 (1995).
14. T. V. Ramakrishnan, C. M. Varma, *Phys. Rev. B* **24**, 137 (1981).
15. Y. De Wilde *et al.*, *Phys. Rev. Lett.* **78**, 4273 (1997).
16. K. O. Cheon *et al.*, *Phys. Rev. B* **58**, 6463 (1998).
17. P. C. Canfield *et al.*, *J. Appl. Phys.* **70**, 5800 (1991). Z. Fisk *et al.*, *Phys. Rev. Lett.* **67**, 3310 (1991).